Induction of Endoplasmic Reticulum Stress Genes, *BiP* and *Chop*, in Genetic and Environmental Models of Retinal Degeneration

Heike Kroeger,[1] *Carissa Messah,*[1] *Kelly Ahern,*[2] *Jason Gee,*[2] *Victory Joseph,*[1] *Michael T. Matthes,*[2] *Douglas Yasumura,*[2] *Marina S. Gorbatyuk,*[3] *Wei-Chieh Chiang,*[1] *Matthew M. LaVail,*[2] and *Jonathan H. Lin*[1]

Purpose. Endoplasmic reticulum (ER) stress has been observed in animal models of retinitis pigmentosa expressing P23H rhodopsin. We compared levels of tightly induced ER stress genes, *Binding of immunoglobulin protein (BiP)* and *CCAAT/enhancer-binding protein homologous protein (Chop)*, in seven additional models of retinal degeneration arising from genetic or environmental causes.

Methods. Retinas from transgenic S334ter rhodopsin (lines 3, 4, and 5) and Royal College of Surgeons (RCS and RCS-*p*+) rats from postnatal (P) days 10 to 120 were analyzed. In a constant light (CL) model of retinal degeneration, BALB/c mice were exposed to 15,000 lux of CL for 0 to 8 hours. Retinal tissues from three to eight animals per experimental condition were collected for histologic and molecular analyses.

Results. S334ter animals revealed significant increases in *BiP*, S334ter-3 (3.3× at P15), S334ter-4 (4× at P60), and S334ter-5 (2.2× at P90), and *Chop*, S334ter-3 (1.3× at P15), S334ter-4 (1.5× at P30), and S334ter-5 (no change), compared with controls. P23H-3 rats showed significant increase of *BiP* at P60 (2.3×) and *Chop* (1.6×). RCS and RCS-*p*+ rats showed significant increases in *BiP* at P60 (2.4×) and P20 (1.8×), respectively, but no statistically significant changes in *Chop*. BALB/c mice showed increases in *BiP* (1.5×) and *Chop* (1.3×) after 4 hours of CL. Increased levels of these ER stress markers correlated with photoreceptor cell loss.

Conclusions. Our study reveals surprising increases in *BiP* and to a lesser degree *Chop* in retinal degenerations arising from diverse causes. We propose that manipulation of ER stress responses may be helpful in treating many environmental and heritable forms of retinal degeneration. (*Invest Ophthalmol Vis Sci.* 2012;53:7590–7599) DOI:10.1167/iovs.12-10221

From the [1]Department of Pathology, University of California, San Diego, La Jolla, California; the [2]Department of Ophthalmology, University of California-San Francisco, San Francisco, California; and the [3]Department of Cell Biology and Anatomy, University of North Texas Health Science Center, Fort Worth, Texas.

Supported by grants from the National Institute of Health (EY001919, EY002162, EY006842, EY018313, EY020846, EY020905), Hope for Vision, Research to Prevent Blindness, and the Foundation Fighting Blindness.

Submitted for publication May 18, 2012; revised September 13 and September 27, 2012; accepted September 27, 2012.

Disclosure: **H. Kroeger**, None; **C. Messah**, None; **K. Ahern**, None; **J. Gee**, None; **V. Joseph**, None; **M.T. Matthes**, None; **D. Yasumura**, None; **M.S. Gorbatyuk**, None; **W.-C. Chiang**, None; **M.M. LaVail**, None; **J.H. Lin**, None

Corresponding author: Jonathan H. Lin, 9500 Gilman Drive #0612, La Jolla, CA 92093-0612; JLin@ucsd.edu.

The endoplasmic reticulum (ER) is a membranous organelle responsible for the folding and maturation of secretory and membrane proteins, lipid and sterol synthesis, and is a major site of intracellular free calcium storage.[1] Pathologic processes that disrupt ER functions cause ER stress.[2] Many heritable mutations in secretory and membrane proteins cause protein misfolding and ER stress.[3–5] Left uncontrolled, ER stress will ultimately cause cell death.[6] ER stress has been reported in several retinal dystrophies arising from protein misfolding,[7–10] including multiple models of retinal degeneration expressing P23H rhodopsin,[11–13] the most common genetic cause of heritable retinitis pigmentosa in the North American population,[14] as well as T17M rhodopsin and S334ter rhodopsin.[15–17] ER stress has also been reported in retinal degeneration 1 mouse (rd1) strain that bear markedly elevated intracellular calcium levels in photoreceptors,[18] and in a light-induced mouse model of retinal degeneration.[19] These findings suggest that ER stress may be involved in retinal dystrophies arising from causes besides protein misfolding. To examine the involvement of ER stress in different retinal dystrophies in more detail, we analyzed expression levels of two genes that are induced by ER stress, *Binding of immunoglobulin protein (BiP)*, and *CCAAT/enhancer-binding protein homologous protein (Chop)*, in seven different rodent models of retinal degeneration arising from etiologies distinct from ER protein misfolding.

We specifically examined *BiP* and *Chop* because these are two of the best studied genes transcriptionally induced by ER stress, and robust protocols are available to quantify their mRNA levels in individual rodent retinas.[20] *BiP*, also known as *glucose-regulated protein 78kD (Grp78)* and *heat shock 70kDa protein 5* (*HspA5)*, encodes an abundant, ER-localized HSP70-class chaperone that participates in protein folding in the ER and binding to misfolded ER proteins for further quality control/triage.[21–23] Cells rapidly upregulate *BiP* mRNA levels when confronted with ER stress.[24,25] Translation of *BiP* mRNA is further regulated by an internal ribosomal entry site located in 5′ untranslated region (UTR) of the mRNA.[26] Elevated *BiP* mRNA levels are a sensitive indicator of ER stress and have been observed in diseases linked to ER stress[27–29] and in retinal degeneration models arising from P23H rhodopsin expression.[12,13] BiP helps cells to cope with ER stress, in part, by reducing levels of misfolded intermediates in the ER.[2,30] In the retina, BiP localizes to the inner segment, where the ER is found.[18,31] Other researchers additionally found BiP in the outline of the inner nuclear layer (ER membrane and nucleus membrane are connected), inner plexiform layer, and the inner segment.[18,19] BiP has been reported to interact with rhodopsin,[32] and with proapoptotic proteins, such as procaspase 7, procaspase 12, and Bcl-2-interacting killer (BiK).[13,33,34] Intrigu-

Investigative Ophthalmology & Visual Science, November 2012, Vol. 53, No. 12

ingly, viral transduction of BiP into rodent photoreceptors expressing P23H rhodopsin significantly improved visual function.[13] Mice lacking *BiP* die during early embryogenesis (E3.5) underscoring BiP's importance in cellular functions essential for survival.[35]

Another well-studied gene transcriptionally induced by ER stress is *Chop*, also known as *Growth arrest and DNA damage gene 153 (Gadd153)* and *DNA damage-inducible transcript 3* (*Ddit3*).[36] *Chop* encodes a transcription factor that promotes apoptosis in response to uncontrolled ER stress.[6,37] The CHOP protein heterodimerizes with other bZIP transcription factors including C/EBPα, C/EBPγ, C/EBPβ, C/EBPε, ATF-4, and p21SNFT.[38,39] For example, under ER stress condition, CHOP interacts with liver inhibitory protein (LIP), a C/EBPβ isoform, to form a heterodimer.[40] Upon heterodimerizatiion, CHOP is transported to the nucleus and induces ER stress-caused apoptosis.[40] Elevated *Chop* mRNA levels have been identified in diseases associated with ER stress including in several animal models of retinal degeneration.[10,12,13,41,42] Cells lacking *Chop* are resistant to many ER stress-inducing insults underscoring Chop's pro-apoptotic capabilities.[41,43,44] Interestingly, reduction in Chop levels, seen after BiP overexpression, correlated with improved visual function in animals expressing misfolded P23H rhodopsin.[13]

In this study, we analyzed retinal degeneration models arising from etiologies mechanistically distinct from ER protein misfolding that included three lines of transgenic S334ter rhodopsin rats with different rates of retinal degeneration[45]; Royal College of Surgeons (RCS) rats in pink-eyed and pigmented backgrounds both with defective rod outer segment phagocytosis by retinal pigment epithelium (RPE)[46–48]; and BALB/c mice acutely exposed to strong light. We measured *BiP* and *Chop* levels in individual retinas from animals at time points before, and during early and late phases of retinal degeneration. Here, we report an unexpected increase in the expression of both ER stress biomarkers in all animal models studied, including S334ter rhodopsin rats, RCS rats, and in a BALB/c mouse model of acute light-induced retinal degeneration compared with controls. The onset of *BiP* and *Chop* expression tightly correlated with retinal degeneration in all models. Our findings reveal that ER stress is a common intracellular signaling mechanism activated during retinal degeneration and may contribute to the pathogenesis of many types of retinal dystrophies.

Methods

Animals and Histologic Analyses

All studies were conducted in accordance with the ARVO Statement for the Use of Animals in Ophthalmic and Vision Research and the guidelines of the institutional animal care committees at the University of California, San Francisco, and the University of California, San Diego. S334ter and P23H rhodopsin transgenic rat lines were created previously (http://www.ucsfeye.net/mlavailRDratmodels.shtml).[45,49] We examined retinal tissue from S334ter (lines 3, 4, and 5) and P23H (line 3) transgenic rats mated with wild-type Sprague-Dawley animals at P10, 15, 20, 30, 60, 90, or 120. As controls, we collected retinal tissue from age-matched Sprague-Dawley littermates.

Inbred, pink-eyed RCS and congenic, pigmented RCS-*p*+ rats with inherited retinal dystrophy were characterized previously[46,50–52] (http://www.ucsfeye.net/mlavailRDratmodels.shtml). We collected retinal tissue from RCS and RCS-*p*+ animals at P10, 12, 20, 30, 45, 60, and 90. As controls, we collected retinal tissue from wild-type age-matched RCS-*rdy*+ rats.

BALB/c mice retinal tissue was collected for histologic and molecular analyses after constant light exposure. As controls, we collected retinal tissue from BABL/c mice without constant light (CL) exposure. For histologic studies, animals were euthanized and perfusion-fixed. Eyes were bisected, post-fixed, and embedded in an epoxy resin as described.[45,46] One micrometer-thick sections were cut through the optic nerve head and stained with Toluidine Blue. To quantify outer nuclear layer (ONL) thickness, nine 440-μm adjacent fields on each side of the optic nerve head were measured. Three measurements of the ONL thickness were made in each field to obtain a mean thickness for each field.[53] The average ONL thickness with SD for each field was based on measurements from at least three animals in each experimental cohort.

Constant Light Damage

For the BALB/c albino mice constant light study, BALB/c mice were dark adapted for 16 hours prior to exposure to 15,000 lux of constant fluorescence light for 0, 1, 2, 4, or 8 hours. Retinal tissues were collected immediately after light exposure for molecular or histologic analysis. For each animal, one eye was used for histologic studies, and the other eye was used for molecular analysis.

Molecular Analyses of *BiP* and *Chop* in Retina

Retinas from three to eight animals per experimental condition were individually collected for molecular analyses to quantify *BiP* and *Chop* mRNA levels. RNA was extracted from individual retinas (RNeasy mini kit; Qiagen, Hilden, Germany). cDNA was generated from total RNA (iScript cDNA synthesis kit; Bio-Rad, Hercules, CA). Quantitative PCR analysis was performed as previously described.[20] *Ribosomal protein L19 (Rpl19)* mRNA levels were measured as a housekeeping gene to verify the quality of the qPCR.

PCR primers used include: rat *Rpl19*: 5′-TGGACCCCAATGAAAC CAAC-3′ and 5′ TACCCTTCCTCTTCCCTATGCC-3′; mouse *Rpl19*: 5′-ATGCCAACTCCCGTCAGCAG-3′ and 5′-TCATCCTTCTCATCCAGGT-CACC-3′, mouse/rat *BiP*: 5′-CCTGCGTCGGTGTGTTCAAG-3′ and 5′-AAGGGTCATTCCAAGTGCG-3′; mouse/rat *Chop*: 5′-ACGGAAACA GAGTGGTCAGTGC-3′ and 5′-CAGGAGGTGATGCCCACTGTTC-3.′

Biochemistry

Wild-type, P23H, or S334ter rhodopsins were transfected into HEK293 cells (Lipofectamine 2000 transfection reagent; Invitrogen, Carlsbad, CA) and lysates were collected (2% SDS, 62.5 mM Tris-HCl pH 6.8, protease inhibitors [Sigma-Aldrich, St. Louis, MO]). Total protein was separated by SDS-PAGE followed by Western blot analysis using the following antibodies: 1D4 anti-rhodopsin at 1:1000 (Santa Cruz Biotechnologies, Santa Cruz, CA); R2-12 anti-rhodopsin at 1:1000 (gift of W.C. Smith, University of Florida); anti-Glyceraldehyde 3-phosphate dehydrogenase (GAPDH) at 1:5000 (Santa Cruz Biotechnologies). After incubation with primary antibody, membranes were washed and incubated in a horseradish peroxidase-coupled secondary antibody (Promega, Madison, WI) at 1:5000 dilution. Immunoreactivity was detected using the SuperSignal West Dura chemiluminescent substrate (Pierce, Rockford, IL).

Rat retinas were lysed in 300-μL lysis buffer (PBS, 0.5 g/mL n-Dodecyl-beta-D-Maltoside [Calbiochem EMD Bioscience, Darmstadt, Germany], protease- [Roche Diagnostic, Indianapolis, IN], and phosphatase inhibitor [Thermo Scientific, Rockford, IL] and sonicated [3× 5 seconds]). Retinal protein lysate concentrations were measured using bicinchoninic acid assay (BCA; Pierce). Total protein was separated by SDS-PAGE followed by Western blot analysis using the following antibodies: anti-Grp78/BiP at 1:1000 (GeneTex, Irvine, CA), anti-GADD153/CHOP at 1:1000 (GeneTex) and anti-Hsp90 as loading control at 1:1000 (GeneTex). After incubation with the primary antibody, membranes were washed and incubated in a horseradish peroxidase-coupled rabbit secondary antibody (Santa Cruz Biotechnologies) at 1:7000 dilution. Immunoreactivity was detected using the

SuperSignal West Pico and SuperSignal West Femto chemiluminescent substrate (Pierce).

Statistical Analyses

All results are presented as mean ±SD from at least three to eight individual animals per experimental condition. Student's two-tailed *t*-tests were performed to determine *P* values for paired groups. A value of $P < 0.05$ was considered significant.

Results

BiP and *Chop* Expression in Mutant Rhodopsin Rats

The S334ter rhodopsin mutation causes premature truncation of mouse opsin and leads to retinal degeneration.[49,54] By contrast to "Class II" rhodopsin mutations such as P23H rhodopsin that misfold and aggregate, S334ter rhodopsin does not aggregate into dimers/oligomers and instead, shows protein mobility similar to wild-type (WT) rhodopsin on SDS-PAGE (see Supplementary Material and Supplementary Fig. S1, http://www.iovs.org/lookup/suppl/doi:10.1167/iovs.12-10221/-/DCSupplemental).[17] The truncated S334ter protein lacks the last 15 amino acid residues that are needed for proper intracellular trafficking of rhodopsin proteins and phototransduction attenuation.[49,54,55] It is unknown if abnormalities in rhodopsin protein trafficking or phototransduction trigger ER stress. We analyzed three different lines (S334ter-3, S334ter-4, and S334ter-5) of transgenic rats expressing S334ter that show distinct rates of retinal degeneration.[45] For example, by P30, S334ter-3 rats show approximately 90% reduction in ONL thickness; S334ter-4 rats show approximately 20% reduction in ONL thickness; and S334ter-5 rats show approximately 60% reduction in ONL thickness when compared with wild-type age-matched Sprague-Dawley rats (Figs. 1A, 1C, 1E).[45]

We analyzed retinas from S334ter-3 rats at P10, 15, 30, and 60. Our prior studies showed that the ONL is indistinguishable in thickness between S334ter-3 and wild-type littermates at P10, but starts to diminish in size at P15.[45] We found no difference in *BiP* and *Chop* mRNA levels between S334ter-3 and wild-type rats collected from P10 animals (Figs. 1A, 1B, and Table). However, we found strong increases in *BiP* mRNA levels at all other ages examined (P15, 30, and 60) (Fig. 1A and Table). The most significant change in *BiP* mRNA level was detected at P15 (~3.3-fold increase, $P = 1.40E\text{-}06$), when compared with retinas from age-matched controls. We also identified increases in *Chop* mRNA levels at P15 and 60 when compared with age-matched littermate controls (Fig. 1B and Table).

Retinas from S334ter-4 rats were analyzed at P10, 20, 30, 60, and 120. Our prior studies showed that the ONL is indistinguishable between S334ter-4 and wild-type animals at P10 and starts to diminish in size at P20.[45] We found no difference in *BiP* and *Chop* mRNA levels between S334ter-4 and wild-type littermates at P10. However, we found significant increases in *BiP* mRNA levels at all other ages examined (P20, 30, 60, and 120), with the strongest change at P60 (~4-fold increase, $P = 9.40E\text{-}06$), when compared with retinas from age-matched controls. Significant increases of *Chop* mRNA levels were also detected at P20 and P30 when compared with age-matched controls (Figs. 1C, 1D, and Table). When we analyzed total retina protein lysates from S334ter-4 animals, we also found increased BiP protein at P10 and CHOP protein at P30 compared with Sprague-Dawley controls at equivalent ages (Figs. 2A–D).

We further analyzed retinas from S334ter-5 rats at P10, 20, 30, 60, and 90. Previous results showed that ONL is indistinguishable between S334ter-5 and wild-type littermates at P10 and starts to diminish in size at P20.[45] We found no increase in *BiP* and *Chop* mRNA levels between S334ter-5 and wild-type littermates at P10. However, we found significant increases in *BiP* mRNA levels at P20, 60, and 90 when compared with age-matched controls (Fig. 1E and Table). When we analyzed total retina protein lysates from S334ter-5 animals, we also found increased BiP protein at P10 and P60 and CHOP protein at P10 compared with Sprague-Dawley controls at equivalent ages (Figs. 2A, 2B and Figs. 2E, 2F).

We previously saw increased *BiP* and *Chop* mRNA expression in vitro and in animals expressing P23H rhodopsin.[12,13] For comparison with our current S334ter rhodopsin transgenic animals, we also analyzed retinas from transgenic rats expressing mutant P23H rhodopsin at P10, 15, 30, and 60. Consistent with prior reports, we found significant increases in *BiP* and *Chop* mRNA in these animals at P15 and P60 when compared to age-matched controls (Figs. 1G, 1H, and Table), which correlates with the occurrence of retinal degeneration as visualized by the decrease of the ONL (Fig. 1G). Intriguingly, the increase in *BiP* and *Chop* mRNA was comparable between P23H and S334ter lines despite the distinct molecular and cellular behavior of the individual mutant rhodopsins. Overall, these findings reveal an unexpected induction of *BiP* and *Chop* in S334ter-3, S334ter-4, and S334ter-5 retinas and suggest that ER stress contributes to retinal degeneration in these models, even though S334ter rhodopsin mutations are not "Class II" rhodopsin mutations (e.g., P23H rhodopsin). We also observed unexpected induction of BiP and CHOP proteins in the S334ter-4 and S334ter-5 animals, but there was a temporal discordance between *BiP* and *Chop* mRNA and protein levels that could reflect additional levels of translational control of *BiP* and *Chop* mRNAs in retinal cell types, by an internal ribosomal entry site on the *BiP* mRNA[56–59] and an inhibitory 5′ upstream open reading frame on the *Chop* mRNA.[60,61]

BiP and *Chop* Expression in Royal College of Surgeons Rats

RCS rats bear mutations in the *Mertk* receptor tyrosine kinase.[52] By contrast to the P23H or S334ter rhodopsin mutations that lead to expression of abnormal rhodopsin proteins, the *Mertk* mutation that causes retinal dystrophy in RCS animals results in the complete loss of MERTK protein expression.[52] MERTK loss causes defects in photoreceptor rod outer segment phagocytosis by the RPE.[47] The precise signaling processes activated by defective outer segment phagocytosis are not fully understood. The involvement of ER stress in this model is unknown. We examined, if there were alterations in *BiP* and *Chop* mRNA levels using inbred pink-eyed RCS and congenic pigmented RCS-*p*+ animals. Retinas from RCS animals at P10, 12, 20, 30, 45, 60, and 90 were analyzed. Prior histologic studies in RCS animals showed that decreases in ONL did not occur until P20 or later,[46] which was confirmed in our histologic analysis (Figs. 3A, 3C). On the molecular level, we found no increases in *BiP* or *Chop* mRNA at P10 or P12 when there was no retinal degeneration (Figs. 3A, 3B, and Table). Surprisingly, we detected statistically significant increases in *BiP* mRNA at P45, 60, and 90 in RCS animals compared with age-matched RCS-*rdy*+ controls (Fig. 3A and Table). For pigmented RCS-*p*+ animals, we analyzed retinas at P10, 12, 20, 30, 60, and 90. Previous histologic analysis of RCS-*p*+ animals revealed decreases in the ONL after P20.[46,51] We found mild, but statistically significant increases in *BiP* mRNA at P20 and 90, when compared with age-matched

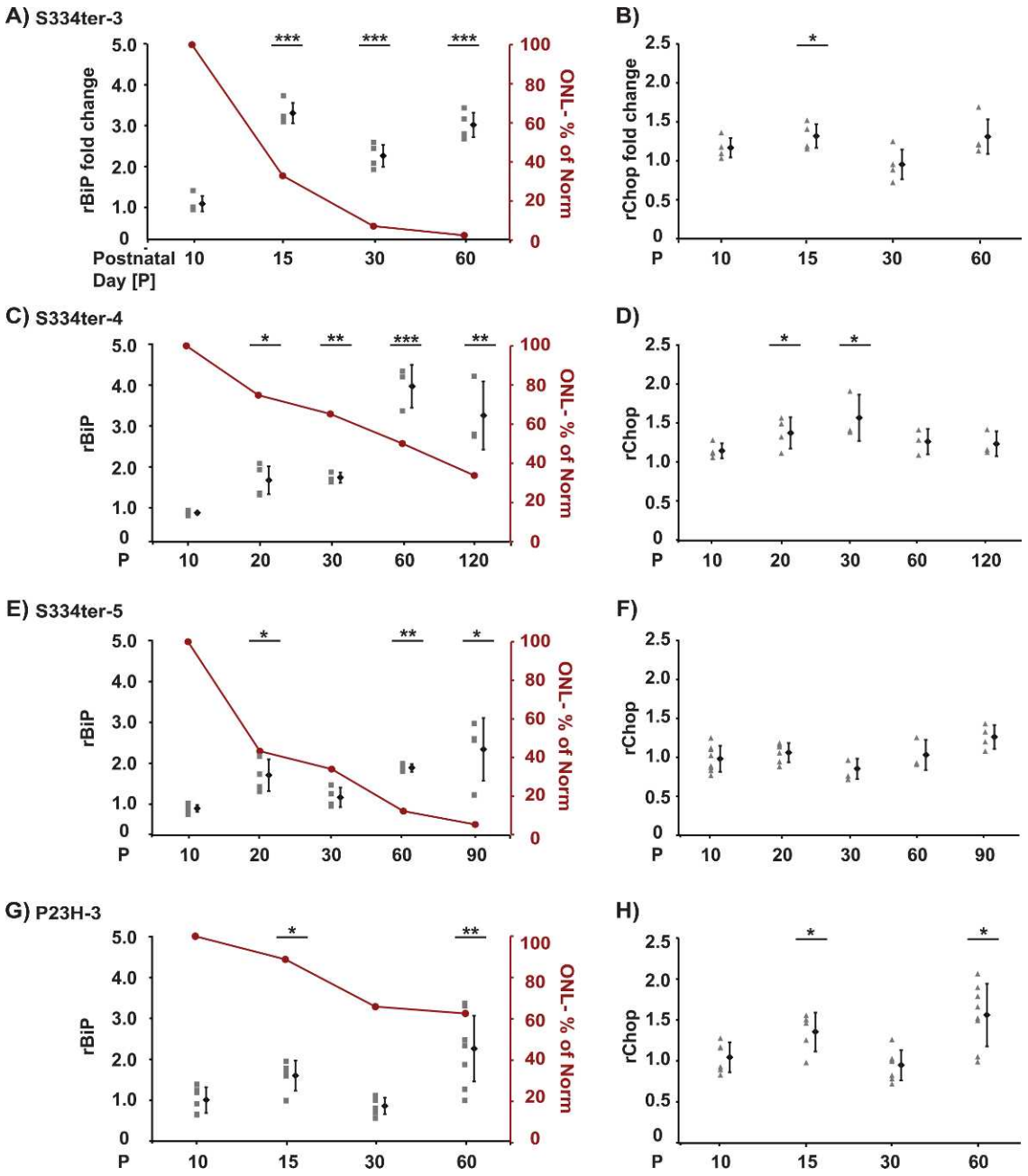

Figure 1. Induction of *BiP* and *Chop* mRNAs in retinas of mutant rhodopsin rats. Analysis of *BiP* and *Chop* mRNA levels by quantitative PCR using rat retina samples at indicated postnatal day ages (P). Samples were plotted relative to the average gene levels at the same age in wild-type Sprague-Dawley control animals. (**A**) *BiP* and (**B**) *Chop* mRNA levels of S334ter-3 animals (**C**) *BiP* and (**D**) *Chop* mRNA levels of S334ter-4 animals. (**E**) *BiP* and (**F**) *Chop* mRNA levels of S334ter-5 animals. (**G**) *BiP* and (**H**) *Chop* mRNA levels of P23H-3 animals. **(A-H)** Retinas from three to eight animals were collected for each postnatal day age (P), and the gene expression level from each animal is plotted individually at each time point. The mean value and SD for the cohort of animals at each time point is plotted to the right. The amount of degeneration is graphically presented as a percent of the normal ONL thickness at each time point as red line for each animal model (**A**, **C**, **E**, **G**). *P* values represent the following asterisk system: $^{*}P < 0.05$, $^{**}P < 0.005$, $^{***}P < 0.0005$.

controls (Fig. 3C and Table). We also observed increases in *Chop* mRNA at P30 and 60 in RCS or RCS-*p*+ animals, respectively, but they were not statistically significant (Figs. 3B, 3D, and Table). These findings indicate that *BiP* mRNA is induced in RCS retinas. By contrast to the S334ter or P23H rhodopsin animals, induction of *BiP* mRNA occurred during later phases of retinal degeneration in RCS animals and not at earlier stages.

BiP and *Chop* Expression in BALB/c Constant Light Model of Retinal Degeneration

Albino animals are susceptible to retinal degeneration from CL exposure, and a prior report had shown increases in several ER stress markers, days after albino BALB/c mice were exposed to constant light.[19] We examined *BiP* and *Chop* levels in retinas of BALB/c mice after 1, 2, 4, or 8 hours of 15,000 lux CL exposure. After 1 or 2 hours of CL, pyknotic

Table. Data Summary of All Animal Models Tested, including Numbers of Animals Used, SD, and Statistical Values

Animal Model	Total *N* of Animals Analyzed for Each Individual Time Point	Time Point	Gene	Mean	SD	*P* Value
S334ter-3	4	P10	rBiP	0.924	0.19	0.5800
		P15	rBiP	3.254	0.26	1.40E–06
		P30	rBiP	2.154	0.28	8.30E–05
		P60	rBiP	2.950	0.32	9.70E–06
		P10	rCHOP	1.120	0.12	0.1766
		P15	rCHOP	1.265	0.15	0.0308
		P30	rCHOP	0.915	0.18	0.4240
		P60	rCHOP	1.257	0.21	0.1207
S334ter-4	3 to 4	P10	rBiP	0.739	0.05	0.0206
		P20	rBiP	1.569	0.35	0.0259
		P30	rBiP	1.634	0.13	0.0010
		P60	rBiP	3.965	0.55	9.40E–06
		P120	rBiP	3.220	0.87	0.0006
		P10	rCHOP	1.098	0.09	0.1809
		P20	rCHOP	1.317	0.19	0.0186
		P30	rCHOP	1.501	0.28	0.0053
		P60	rCHOP	1.211	0.16	0.1853
		P120	rCHOP	1.185	0.15	0.2381
S334ter-5	3 to 8	P10	rBiP	0.693	0.09	0.0011
		P20	rBiP	1.550	0.41	0.0195
		P30	rBiP	0.982	0.25	0.8978
		P60	rBiP	1.742	0.10	0.0028
		P90	rBiP	2.220	0.81	0.0080
		P10	rCHOP	0.940	0.16	0.4609
		P20	rCHOP	1.013	0.11	0.8692
		P30	rCHOP	0.810	0.13	0.0389
		P60	rCHOP	0.990	0.19	0.9238
		P90	rCHOP	1.200	0.15	0.1422
P23H-3	5 to 8	P10	rBiP	1.009	0.31	0.9562
		P15	rBiP	1.605	0.37	0.0106
		P30	rBiP	0.864	0.20	0.2276
		P60	rBiP	2.265	0.80	0.0048
		P10	rCHOP	1.050	0.18	0.6103
		P15	rCHOP	1.357	0.24	0.0138
		P30	rCHOP	0.950	0.19	0.4240
		P60	rCHOP	1.560	0.38	0.0073
RCS	3 to 6	P10	rBiP	0.765	0.20	0.0522
		P12	rBiP	0.994	0.11	0.9703
		P20	rBiP	1.384	0.33	0.0560
		P30	rBiP	1.167	0.11	0.1933
		P45	rBiP	2.028	0.49	0.0248
		P60	rBiP	2.430	0.28	0.0006
		P90	rBiP	1.979	0.26	0.0012
		P10	rCHOP	0.820	0.11	0.0200
		P12	rCHOP	0.920	0.21	0.4010
		P20	rCHOP	1.020	0.06	0.7540
		P30	rCHOP	1.170	0.29	0.3940
		P45	rCHOP	0.850	0.23	0.4930
		P60	rCHOP	0.950	0.15	0.6910
		P90	rCHOP	0.530	0.08	0.0040
RCS-p+	5 to 8	P10	rBiP	0.590	0.15	0.0013
		P12	rBiP	1.460	0.57	0.0741
		P20	rBiP	1.750	0.38	0.0046
		P30	rBiP	1.190	0.21	0.2027
		P60	rBiP	1.480	0.51	0.1269
		P90	rBiP	1.650	0.45	0.0468
		P10	rCHOP	0.4490	0.17	0.0003
		P12	rCHOP	0.9470	0.11	0.3540
		P20	rCHOP	0.6890	0.33	0.0790
		P30	rCHOP	1.0760	0.14	0.4180
		P60	rCHOP	1.0870	0.15	0.4480
		P90	rCHOP	0.6330	0.11	0.0060
BALB-c	4	0 hours	mBiP	1.000	0.27	–
		1 hours	mBiP	1.106	0.21	0.5537
		2 hours	mBiP	1.268	0.38	0.2888
		4 hours	mBiP	1.490	0.23	0.0324
		8 hours	mBiP	1.249	0.33	0.2848
		0 hours	mCHOP	1.000	0.15	–
		1 hours	mCHOP	1.183	0.07	0.0642
		2 hours	mCHOP	1.309	0.14	0.0230
		4 hours	mCHOP	1.331	0.18	0.0285
		8 hours	mCHOP	1.295	0.23	0.0724

	Control Animals		Total Animals	
Animal Model	Total N of Animals Analyzed for Each Individual Time Point	Time Point	Rodent	Total
RCS-rdy+	3 to 8	P10	Mice	53
		P12	Rat	186
		P20		
		P30		
		P45		
		P60		
		P90		
SD controls	5 to 6	P10		
		P15		
		P30		
		P60		

nuclei appeared in the ONL (Figs. 4B, 4C). Furthermore, the thickness of the ONL decreased, and the inner and outer segments were shorter and disorganized after 1 or 2 hours of light injury (Figs. 4B, 4C), with the 2 hour light exposure resulting in the ONL being significantly thinner than the control retinas (Fig. 4A; $P < 0.005$) or those receiving 1 hour of light ($P < 0.01$). This loss of ONL thickness after 2 hours of light exposure is seen in spidergrams of the ONL (Fig. 4F). After 4 or 8 hours of photic injury, increased numbers of pyknotic photoreceptor nuclei were evident accompanied by increased vacuolization and disorganization of the rod inner and outer segments and edematous swelling throughout the ONL (Figs. 4D, 4E). This led the ONL to appear thicker than after 2 hours of light (Fig. 4F). After the longest exposure (8 hours), the ONL was particularly distorted and irregular, with some foci being as thin as 27.1 μm, similar to the left side of Figure 4E, and some regions being as thick as 64.9 μm (not shown), considerably thicker than those of the control retinas. Thus, the nuclear edema after 4 hours (Fig. 4D) and distortion and vacuolization after 8 hours of light (Fig. 4E) explain why the ONL spidergrams do not show a progressive loss of

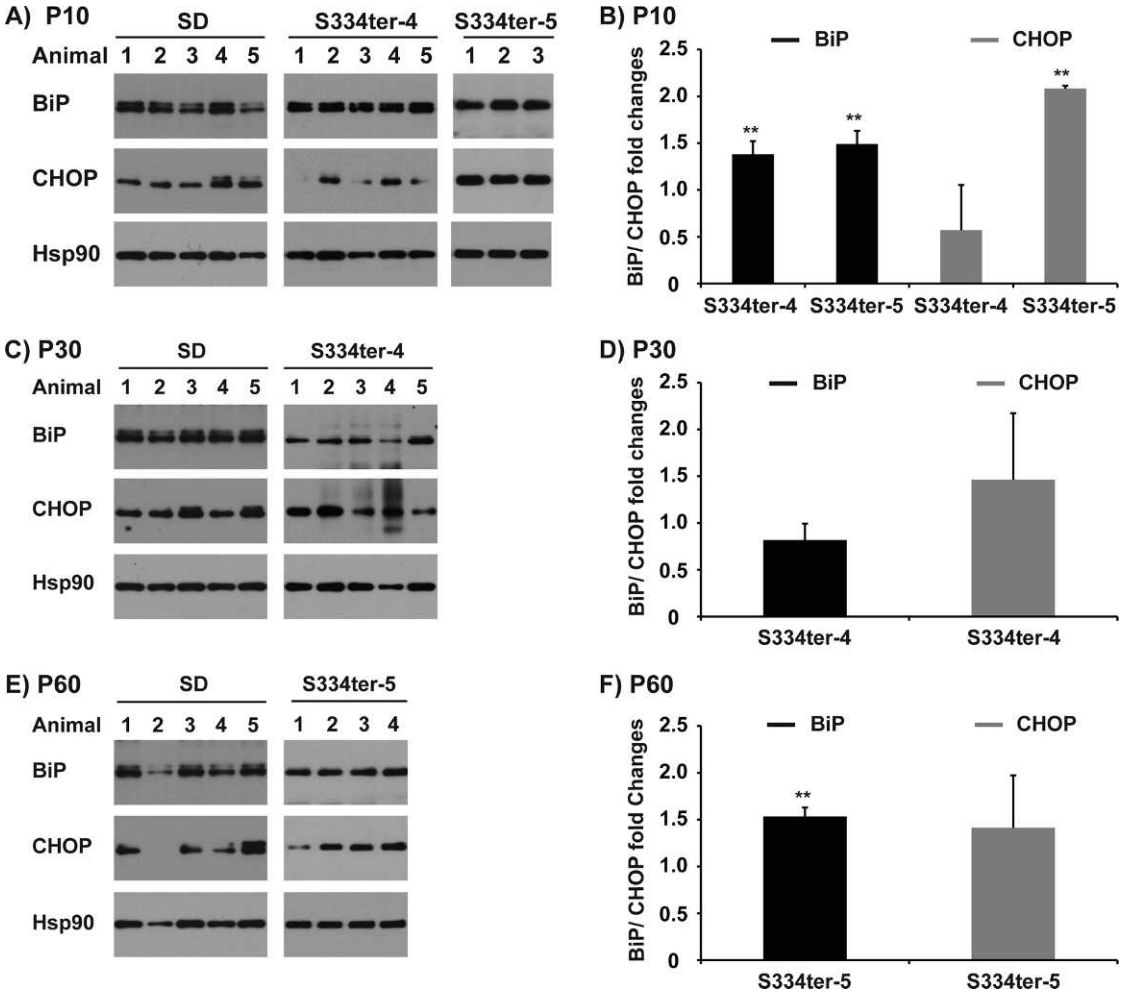

Figure 2. Induction of BiP and CHOP protein in retinas of mutant rhodopsin rats. (**A**) BiP and CHOP protein levels from total retinal protein lysates from three to five Sprague-Dawley, S334ter-4, and S334ter-5 rats at postnatal day 10 (P10) were examined by immunoblotting. Mean value and SD of BiP or CHOP protein levels in S334ter-4 and S334ter-5 cohorts at P10 relative to age-matched Sprague-Dawley controls are plotted in (**B**). (**C**) BiP and CHOP protein levels from total retinal protein lysates from five Sprague-Dawley or S334ter-4 at P30 were examined by immunoblotting. Mean value and SD of *BiP* and *CHOP* protein levels in S334ter-4 cohorts at P30 relative to Sprague-Dawley controls are plotted in (**D**). (**E**) BiP and CHOP protein levels from total retinal protein lysates from four to five Sprague-Dawley or S334ter-5 rats at postnatal day P60 were examined by immunoblotting. Mean value and SD of BiP and CHOP protein levels in S334ter-5 cohorts at P60 relative to Sprague-Dawley controls are plotted in (**F**). **(A**, **C**, **E)** HSP90 protein levels are shown as loading control. *P* values represent the following asterisk system: $^{**}P < 0.005$

thickness with increasing exposure time (Fig. 4F), and why only the 2 hour exposure resulted in statistically different ONL thicknesses from one another; none of the other comparisons of mean ONL thickness was $P < 0.05$. All these durations of photic injury also caused pronounced retinal degeneration when the retinas of animals were examined at 1, 2, and 4 days (>50% reduction in ONL thickness, data not shown).

On a molecular level, we observed mild but statistically significant increases in both *BiP* and *Chop* after 2 and 4 hours of CL exposure, compared with animals that were not exposed to light (Figs. 4G, 4H). These findings indicate that *BiP* and *Chop* are induced acutely during photic injury in BALB/c mice and suggest that ER stress may contribute to retinal degeneration associated with acute phototoxic injury to the retina. By contrast to the molecular and histologic changes we observed in BALB/c mice after CL exposure, pigmented C57/B6 mice exposed to the same CL did not undergo retinal degeneration and showed no changes in *BiP* and *Chop* levels acutely or any time afterward (data not shown), suggesting that the dysregulation seen with *BiP* and *Chop* in BALB/c were linked to the acute retinal damage caused by CL.

Discussion

Prior studies have reported induction of *BiP*, *Chop*, and other markers of ER stress in animal models of retinitis pigmentosa arising from misfolded P23H rhodopsin expression in the retina.[12,13] This builds on extensive in vitro data demonstrating that the P23H and other "Class II" rhodopsin missense mutations cause misfolding, retention in the ER and ER stress.[62,63] Our findings reveal an unexpected induction of *BiP* and *Chop* in several additional models of retinal degeneration arising from causes besides primary ER protein misfolding, including defective rhodopsin protein intracellular trafficking and/or disruption of visual signal transduction in the case of S334ter rhodopsin,[49,54,55] disruption of rod outer segment renewal in the case of RCS animals,[47] and phototoxicity. Intriguingly, dysregulation of *BiP* and *Chop* broadly correlated with loss of ONL thickness in all animals suggesting

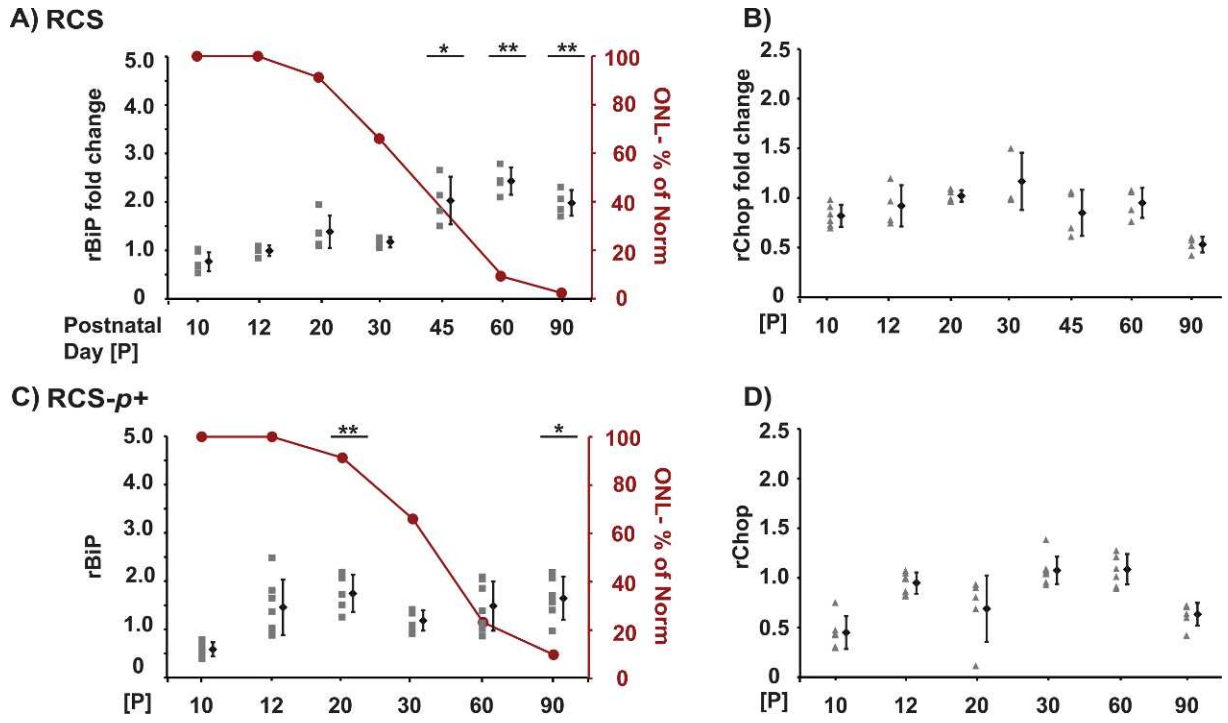

Figure 3. Induction of *BiP* and *Chop* in retinas of RCS rats. Analysis of *BiP* and *Chop* mRNA levels by quantitative PCR using rat retinas at indicated postnatal day ages (P). Samples were plotted relative to average of gene levels of wild-type RCS-*rdy*+ control animals at the same age. (**A**) *BiP* and (**B**) *Chop* mRNA levels of RCS animals. (**C**) *BiP* and (**D**) *Chop* mRNA levels of RCS-*p*+ animals. **(A–D)** Retinas from three to eight animals were collected for each postnatal day age, and the gene expression level from each animal is plotted individually at each time point. The mean value and SD for the cohort of animals at each time point are plotted to the *right*. The amount of degeneration is graphically presented as a percent of the normal ONL thickness at each time point as *red line* for each animal model (**A**, **C**). *P* values represent the following asterisk system: $^{*}P < 0.05$, $^{**}P < 0.005$.

a link between ER dysregulation and the onset or progression or retinal degeneration. How can such diverse insults converge in the induction of *BiP* and *Chop* in the retina? For the S334ter transgenic rats, the truncation removes the 15 carboxy-terminus residues from rhodopsin leading to the mislocalization of a substantial fraction of S334ter rhodopsin to rod inner segment membranes,[49,54] as well as deleting amino acid residues in rhodopsin's carboxyl tail required for terminating the phototransduction cascade.[55] S334ter rhodopsin could directly induce the transcription of *BiP* and *Chop* by causing ER stress after its mislocalization to the inner segment. S334ter rhodopsin could also indirectly cause ER stress by disrupting photoreceptor intracellular calcium homeostasis if the visual cycle cannot be terminated. Indeed, among all the animal models of retinal degeneration we examined, we consistently observed the greatest degree of *BiP* and *Chop* induction in S334ter animals underscoring S334ter rhodopsin's potency in eliciting ER stress. We also observed dysregulation of ER stress markers in the S334ter-4 line previously, albeit with differences in the timing of *BiP* and *Chop* dysregulation that may reflect differences in the environmental conditions under which the studies were performed.[15]

For RCS rats, the failure of the RPE to phagocytize photoreceptor rod outer segments interrupts the normal renewal of photoreceptor outer segments and causes the accumulation of outer segment debris in the subretinal space.[47] The specific signaling mechanisms triggered by these events within photoreceptors that lead to their demise in RCS animals are unclear. However, it is likely that ER functions are compromised when photoreceptor metabolism is impaired, and consequently, ER stress is induced. By contrast to the S334ter rhodopsin animals, we observed a significant induction of *BiP* but not *Chop*. Our findings suggest that other mechanisms are triggered during initial stages of retinal damage in RCS animals while ER stress arises later on and could further amplify the intracellular damage that culminates in photoreceptor cell death. Photoreceptor damage also triggers inflammatory responses and glia activation in the remaining retina, and ER stress changes could also originate from these nonphotoreceptor cell types.[64]

In albino models of phototoxicity, multiple molecular mechanisms have been implicated in retinal degeneration induced by CL.[65] During the acute period of light exposure itself, increased intracellular calcium levels and oxidative stress has been reported,[65] while after light exposure ceases, transcription factors such as c-fos and AP-1 are required to further drive light-induced retinal degeneration several days after the photic injury event.[66–68] Intracellular calcium dysregulation and oxidative stress both disrupt ER functions and induce ER stress. Consistent with this, we observed increased *BiP* and *Chop* shortly after light exposure (2 and 4 hours, Figs. 4G, 4H). Our findings are also in good agreement with a prior report from Tso and colleagues[19] that also observed increased *BiP* early during constant light exposure (3 and 6 hours). Interestingly, Tso and colleagues[19] observed no sustained increase in *BiP* after cessation of light, but instead, they found evidence of activation of other ER stress activated proteins, caspase-12 and phospho-PERK, several days after cessation of light exposure suggesting that other ER stress genes may be involved during later chronic phases of phototoxicity.

Multiple strategies have been proposed to reduce ER stress. Chemical chaperones including retinoids and genetic chaperones have shown efficacy in enhancing rhodopsin folding and/

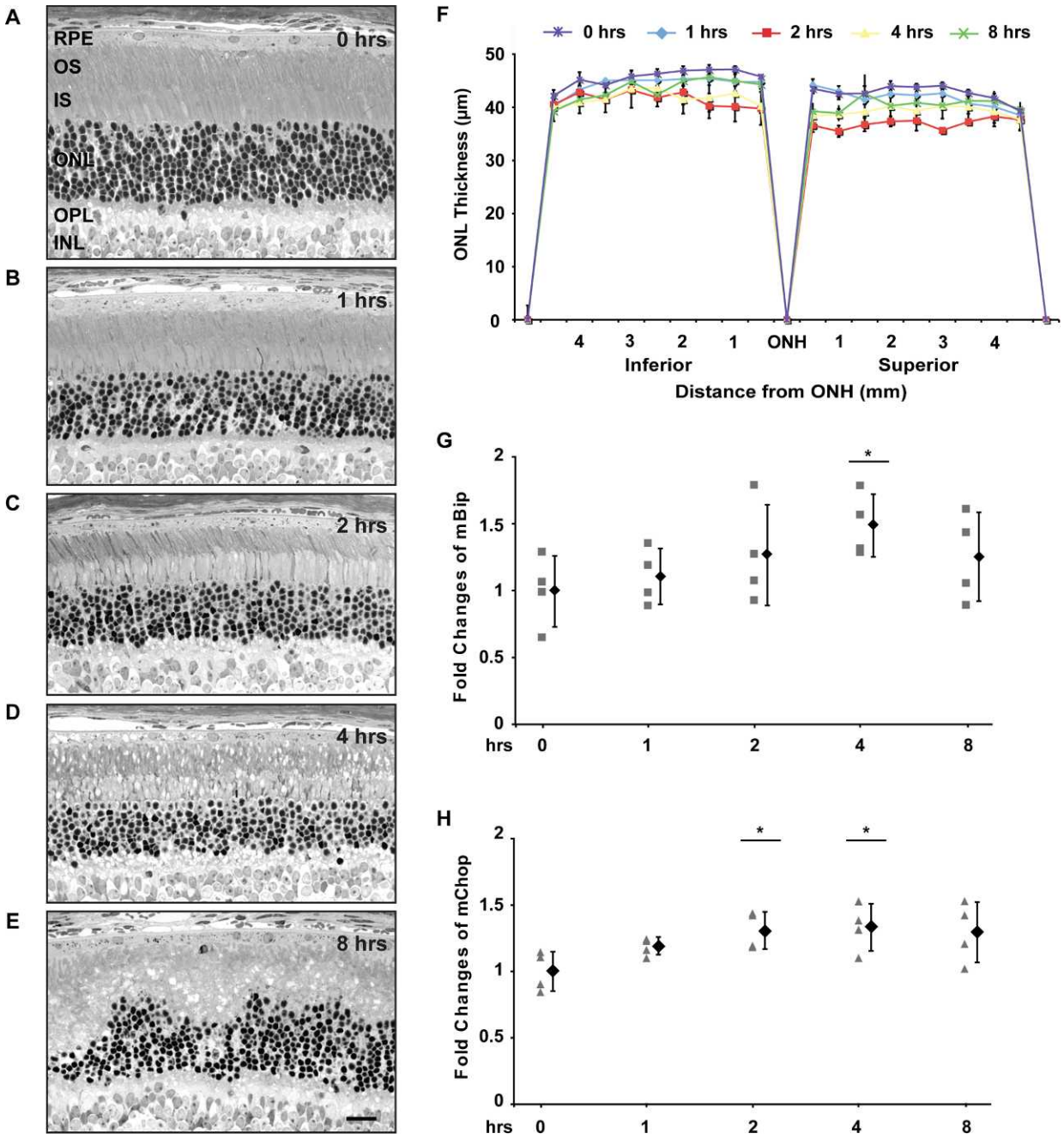

Figure 4. Induction of *BiP* and *Chop* in retinas of BALB/c mice exposed to constant light. Light micrograph of representative retinal section from the inferior posterior retina of BALB/c mice; (**A**) control BALB/c mice, (**B**) 1 hour, (**C**) 2 hours, (**D**) 4 hours, (**E**) 8 hours of CL. (**F**) Thickness of ONL in BALB/c mice exposed to CL for indicated durations. Measurements of the ONL thickness at indicated intervals from optic nerve head to superior and inferior poles from three different animals were collected at each constant light condition, and the mean values are plotted. *Vertical bar* indicates SD. Note, that all of these values are relatively similar, since a single rod photoreceptor nucleus is approximately 4.5 μm in diameter; the mean ONL thickness for the groups that are significantly different ($P < 0.05$) are the 2 hour light exposure compared with controls and with the 1 hour group. **(G, H)** Retinas from four mice were collected at indicated times points; gene expression levels of *BiP* (**G**) and *Chop* (**H**) were measured by quantitative PCR and are presented as relatives to the average levels of mice at time 0. Each animal is plotted individually. The mean value and SD for the cohort of animals is plotted to the *right* at each time point. *P* values represent the following asterisk system: $^*P < 0.05$. INL, inner nuclear layer; IS, inner segments; OPL, outer plexiform layer; OS, outer segments; *Magnification bar* for **A**–**E** = 20 μm.

or preventing protein aggregation.[13,69–72] BiP overexpression in retina enhanced visual function in P23H animals through mechanisms that could involve modulation of ER stress levels and/or protein aggregation.[13] Chemical-genetic approaches to activate ER protein quality control pathways controlled by the unfolded protein response promote misfolded protein degradation in the cell.[17,73] Nontargeted approaches that globally prevent oxidative stress, stabilize proteins, enhance lipid/sterol metabolism, or provide neurotrophic support (e.g., Ciliary neurotrophic factor [CNTF], leukemia inhibitory factor [LIF])[74,75] may also reduce ER stress. Our identification of the induction of ER stress genes in many different models of retinal degeneration suggests that ER stress may be an important common mechanism in retinal degeneration. Ther-

apies that reduce ER stress or upregulate ER stress-induced protective molecules and chaperones in the retina could be beneficial in preserving vision.

References

1. Alberts B. *Molecular Biology of the Cell*. New York: Garland Science; 2008.
2. Walter P, Ron D. The unfolded protein response: from stress pathway to homeostatic regulation. *Science*. 2011;334:1081–1086.
3. Hetz C. The unfolded protein response: controlling cell fate decisions under ER stress and beyond. *Nat Rev Mol Cell Biol*. 2012;13:89–102.
4. Lin JH, Walter P, Yen TS. Endoplasmic reticulum stress in disease pathogenesis. *Annu Rev Pathol*. 2008;3:399–425.
5. Tsang KY, Chan D, Bateman JF, Cheah KS. In vivo cellular adaptation to ER stress: survival strategies with double-edged consequences. *J Cell Sci*. 2010;123:2145–2154.
6. Tabas I, Ron D. Integrating the mechanisms of apoptosis induced by endoplasmic reticulum stress. *Nat Cell Biol*. 2011; 13:184–190.
7. Frederick JM, Krasnoperova NV, Hoffmann K, et al. Mutant rhodopsin transgene expression on a null background. *Invest Ophthalmol Vis Sci*. 2001;42:826–833.
8. Liu H, Wang M, Xia CH, et al. Severe retinal degeneration caused by a novel rhodopsin mutation. *Invest Ophthalmol Vis Sci*. 2010;51:1059–1065.
9. Lin JH, Lavail MM. Misfolded proteins and retinal dystrophies. *Adv Exp Med Biol*. 2010;664:115–121.
10. Karan G, Yang Z, Howes K, et al. Loss of ER retention and sequestration of the wild-type ELOVL4 by Stargardt disease dominant negative mutants. *Mol Vis*. 2005;11:657–664.
11. Tam BM, Moritz OL. Characterization of rhodopsin P23H-induced retinal degeneration in a Xenopus laevis model of retinitis pigmentosa. *Invest Ophthalmol Vis Sci*. 2006;47: 3234–3241.
12. Lin JH, Li H, Yasumura D, et al. IRE1 signaling affects cell fate during the unfolded protein response. *Science*. 2007;318:944–949.
13. Gorbatyuk MS, Knox T, LaVail MM, et al. Restoration of visual function in P23H rhodopsin transgenic rats by gene delivery of BiP/Grp78. *Proc Natl Acad Sci U S A*. 2010;107:5961–5966.
14. Berson EL. Retinitis pigmentosa. The Friedenwald Lecture. *Invest Ophthalmol Vis Sci*. 1993;34:1659–1676.
15. Shinde VM, Sizova OS, Lin JH, Lavail MM, Gorbatyuk MS. ER Stress in Retinal Degeneration in S334ter Rho Rats. *PLoS One*. 2012;7:e33266.
16. Kunte MM, Choudhury S, Manheim JF, et al. ER stress is involved in T17M rhodopsin-induced retinal degeneration. *Invest Ophthalmol Vis Sci*. 2012;53:3792–3800.
17. Chiang WC, Hiramatsu N, Messah C, Kroeger H, Lin JH. Selective activation of ATF6 and PERK endoplasmic reticulum stress signaling pathways prevent mutant rhodopsin accumulation. *Invest Ophthalmol Vis Sci*. 2012;53:7159–7166.
18. Yang LP, Wu LM, Guo XJ, Tso MO. Activation of endoplasmic reticulum stress in degenerating photoreceptors of the rd1 mouse. *Invest Ophthalmol Vis Sci*. 2007;48:5191–5198.
19. Yang LP, Wu LM, Guo XJ, Li Y, Tso MO. Endoplasmic reticulum stress is activated in light-induced retinal degeneration. *J Neurosci Res*. 2008;86:910–919.
20. Hiramatsu N, Joseph VT, Lin JH. Monitoring and manipulating mammalian unfolded protein response. *Methods Enzymol*. 2011;491:183–198.
21. Chang HC, Tang YC, Hayer-Hartl M, Hartl FU. SnapShot: molecular chaperones, Part I. *Cell*. 2007;128:212.
22. Bukau B, Weissman J, Horwich A. Molecular chaperones and protein quality control. *Cell*. 2006;125:443–451.
23. Mayer MP, Bukau B. Hsp70 chaperones: cellular functions and molecular mechanism. *Cell Mol Life Sci*. 2005;62:670–684.
24. Kozutsumi Y, Segal M, Normington K, Gething MJ, Sambrook J. The presence of malfolded proteins in the endoplasmic reticulum signals the induction of glucose-regulated proteins. *Nature*. 1988;332:462–464.
25. Yoshida H, Haze K, Yanagi H, Yura T, Mori K. Identification of the cis-acting endoplasmic reticulum stress response element responsible for transcriptional induction of mammalian glucose-regulated proteins. Involvement of basic leucine zipper transcription factors. *J Biol Chem*. 1998;273:33741–33749.
26. Macejak DG, Sarnow P. Internal initiation of translation mediated by the 5′ leader of a cellular mRNA. *Nature*. 1991; 353:90–94.
27. Tsang KY, Chan D, Cheslett D, et al. Surviving endoplasmic reticulum stress is coupled to altered chondrocyte differentiation and function. *PLoS Biol*. 2007;5:e44.
28. Mulhern ML, Madson CJ, Danford A, Ikesugi K, Kador PF, Shinohara T. The unfolded protein response in lens epithelial cells from galactosemic rat lenses. *Invest Ophthalmol Vis Sci*. 2006;47:3951–3959.
29. Lindholm D, Wootz H, Korhonen L. ER stress and neurodegenerative diseases. *Cell Death Differ*. 2006;13:385–392.
30. Pincus D, Chevalier MW, Aragon T, et al. BiP binding to the ER-stress sensor Ire1 tunes the homeostatic behavior of the unfolded protein response. *PLoS Biol*. 2010;8:e1000415.
31. Mohlin C, Johansson K. Death of photoreceptors in organotypic retinal explant cultures: implication of rhodopsin accumulation and endoplasmic reticulum stress. *J Neurosci Methods*. 2011;197:56–64.
32. Athanasiou D, Kosmaoglou M, Kanuga N, et al. BiP prevents rod opsin aggregation. *Mol Biol Cell*. 2012;23:3522–3531.
33. Fu Y, Li J, Lee AS. GRP78/BiP inhibits endoplasmic reticulum BIK and protects human breast cancer cells against estrogen starvation-induced apoptosis. *Cancer Res*. 2007;67:3734–3740.
34. Reddy RK, Mao C, Baumeister P, Austin RC, Kaufman RJ, Lee AS. Endoplasmic reticulum chaperone protein GRP78 protects cells from apoptosis induced by topoisomerase inhibitors: role of ATP binding site in suppression of caspase-7 activation. *J Biol Chem*. 2003;278:20915–20924.
35. Luo S, Mao C, Lee B, Lee AS. GRP78/BiP is required for cell proliferation and protecting the inner cell mass from apoptosis during early mouse embryonic development. *Mol Cell Biol*. 2006;26:5688–5697.
36. Wang XZ, Lawson B, Brewer JW, et al. Signals from the stressed endoplasmic reticulum induce C/EBP-homologous protein (CHOP/GADD153). *Mol Cell Biol*. 1996;16:4273–4280.
37. Zinszner H, Kuroda M, Wang X, et al. CHOP is implicated in programmed cell death in response to impaired function of the endoplasmic reticulum. *Genes Dev*. 1998;12:982–995.
38. Ubeda M, Wang XZ, Zinszner H, Wu I, Habener JF, Ron D. Stress-induced binding of the transcriptional factor CHOP to a novel DNA control element. *Mol Cell Biol*. 1996;16:1479–1489.
39. Newman JR, Keating AE. Comprehensive identification of human bZIP interactions with coiled-coil arrays. *Science*. 2003; 300:2097–2101.
40. Chiribau CB, Gaccioli F, Huang CC, Yuan CL, Hatzoglou M. Molecular symbiosis of CHOP and C/EBP beta isoform LIP contributes to endoplasmic reticulum stress-induced apoptosis. *Mol Cell Biol*. 2010;30:3722–3731.

41. Benavides A, Pastor D, Santos P, Tranque P, Calvo S. CHOP plays a pivotal role in the astrocyte death induced by oxygen and glucose deprivation. *Glia*. 2005;52:261–275.
42. Hu Y, Park KK, Yang L, et al. Differential effects of unfolded protein response pathways on axon injury-induced death of retinal ganglion cells. *Neuron*. 2012;73:445–452.
43. Oyadomari S, Koizumi A, Takeda K, et al. Targeted disruption of the Chop gene delays endoplasmic reticulum stress-mediated diabetes. *J Clin Invest*. 2002;109:525–532.
44. Pennuto M, Tinelli E, Malaguti M, et al. Ablation of the UPR-mediator CHOP restores motor function and reduces demyelination in Charcot-Marie-Tooth 1B mice. *Neuron*. 2008;57:393–405.
45. Pennesi ME, Nishikawa S, Matthes MT, Yasumura D, LaVail MM. The relationship of photoreceptor degeneration to retinal vascular development and loss in mutant rhodopsin transgenic and RCS rats. *Exp Eye Res*. 2008;87:561–570.
46. LaVail MM, Battelle BA. Influence of eye pigmentation and light deprivation on inherited retinal dystrophy in the rat. *Exp Eye Res*. 1975;21:167–192.
47. Nandrot EF, Dufour EM. Mertk in daily retinal phagocytosis: a history in the making. *Adv Exp Med Biol*. 2010;664:133–140.
48. Bok D, Hall MO. The role of the pigment epithelium in the etiology of inherited retinal dystrophy in the rat. *J Cell Biol*. 1971;49:664–682.
49. Green ES, Menz MD, LaVail MM, Flannery JG. Characterization of rhodopsin mis-sorting and constitutive activation in a transgenic rat model of retinitis pigmentosa. *Invest Ophthalmol Vis Sci*. 2000;41:1546–1553.
50. Sidman RL, Pearlstein R, Waymouth C. Pink-eyed dilution (p) gene in rodents: increased pigmentation in tissue culture. *Dev Biol*. 1965;12:93–116.
51. LaVail MM. Photoreceptor characteristics in congenic strains of RCS rats. *Invest Ophthalmol Vis Sci*. 1981;20:671–675.
52. D'Cruz PM, Yasumura D, Weir J, et al. Mutation of the receptor tyrosine kinase gene *Mertk* in the retinal dystrophic RCS rat. *Hum Mol Genet*. 2000;9:645–651.
53. Faktorovich EG, Steinberg RH, Yasumura D, Matthes MT, LaVail MM. Basic fibroblast growth factor and local injury protect photoreceptors from light damage in the rat. *J Neurosci*. 1992;12:3554–3567.
54. Lee ES, Flannery JG. Transport of truncated rhodopsin and its effects on rod function and degeneration. *Invest Ophthalmol Vis Sci*. 2007;48:2868–2876.
55. Chen J, Makino CL, Peachey NS, Baylor D, Simon MI. Mechanisms of rhodopsin inactivation in vivo as revealed by COOH-terminal truncation mutant. *Science*. 1995;267:374–377.
56. Pacheco A, Twiss JL. Localized IRES-Dependent Translation of ER Chaperone Protein mRNA in Sensory Axons. *PLoS One*. 2012;7:e40788.
57. Cho S, Park SM, Kim TD, Kim JH, Kim KT, Jang SK. BiP internal ribosomal entry site activity is controlled by heat-induced interaction of NSAP1. *Mol Cell Biol*. 2007;27:368–383.
58. Fernandez J, Yaman I, Sarnow P, Snider MD, Hatzoglou M. Regulation of internal ribosomal entry site-mediated translation by phosphorylation of the translation initiation factor eIF2alpha. *J Biol Chem*. 2002;277:19198–19205.
59. Yang Q, Sarnow P. Location of the internal ribosome entry site in the 5′ non-coding region of the immunoglobulin heavy-chain binding protein (BiP) mRNA: evidence for specific RNA-protein interactions. *Nucleic Acids Res*. 1997;25:2800–2807.
60. Palam LR, Baird TD, Wek RC. Phosphorylation of eIF2 facilitates ribosomal bypass of an inhibitory upstream ORF to enhance CHOP translation. *J Biol Chem*. 2011;286:10939–10949.
61. Lee HC, Chen YJ, Liu YW, et al. Transgenic zebrafish model to study translational control mediated by upstream open reading frame of human chop gene. *Nucleic Acids Res*. 2011;39:e139.
62. Kaushal S, Khorana HG. Structure and function in rhodopsin. 7. Point mutations associated with autosomal dominant retinitis pigmentosa. *Biochemistry*. 1994;33:6121–6128.
63. Sung CH, Schneider BG, Agarwal N, Papermaster DS, Nathans J. Functional heterogeneity of mutant rhodopsins responsible for autosomal dominant retinitis pigmentosa. *Proc Natl Acad Sci U S A*. 1991;88:8840–8844.
64. Rattner A, Nathans J. The genomic response to retinal disease and injury: evidence for endothelin signaling from photoreceptors to glia. *J Neurosci*. 2005;25:4540–4549.
65. Wenzel A, Grimm C, Samardzija M, Reme CE. Molecular mechanisms of light-induced photoreceptor apoptosis and neuroprotection for retinal degeneration. *Prog Retin Eye Res*. 2005;24:275–306.
66. Hafezi F, Steinbach JP, Marti A, et al. The absence of c-fos prevents light-induced apoptotic cell death of photoreceptors in retinal degeneration in vivo. *Nat Med*. 1997;3:346–349.
67. Wenzel A, Grimm C, Marti A, et al. c-fos controls the "private pathway" of light-induced apoptosis of retinal photoreceptors. *J Neurosci*. 2000;20:81–88.
68. Hao W, Wenzel A, Obin MS, et al. Evidence for two apoptotic pathways in light-induced retinal degeneration. *Nat Genet*. 2002;32:254–260.
69. Kosmaoglou M, Kanuga N, Aguila M, Garriga P, Cheetham ME. A dual role for EDEM1 in the processing of rod opsin. *J Cell Sci*. 2009;122:4465–4472.
70. Noorwez SM, Ostrov DA, McDowell JH, Krebs MP, Kaushal S. A high-throughput screening method for small-molecule pharmacologic chaperones of misfolded rhodopsin. *Invest Ophthalmol Vis Sci*. 2008;49:3224–3230.
71. Noorwez SM, Malhotra R, McDowell JH, Smith KA, Krebs MP, Kaushal S. Retinoids assist the cellular folding of the autosomal dominant retinitis pigmentosa opsin mutant P23H. *J Biol Chem*. 2004;279:16278–16284.
72. Mendes HF, Cheetham ME. Pharmacological manipulation of gain-of-function and dominant-negative mechanisms in rhodopsin retinitis pigmentosa. *Hum Mol Genet*. 2008;17:3043–3054.
73. Chiang WC, Messah C, Lin JH. IRE1 directs proteasomal and lysosomal degradation of misfolded rhodopsin. *Mol Biol Cell*. 2012;23:758–770.
74. Ueki Y, Wang J, Chollangi S, Ash JD. STAT3 activation in photoreceptors by leukemia inhibitory factor is associated with protection from light damage. *J Neurochem*. 2008;105:784–796.
75. Samardzija M, Wariwoda H, Imsand C, et al. Activation of survival pathways in the degenerating retina of rd10 mice. *Exp Eye Res*. 2012;99:17–26.